2026 IEEE/SICE International Symposium on System Integration (SII)
January 11-14, 2026. Cancún, México

Design of a Low-Cost Strain Gauge Array System for Wind Turbine Blade Damage Detection

Ada R. Aster, Gabriel Perez, and Elijah K. Sleasman
(an.ada.poirier@gmail.com, perezgs999@gmail.com, elijah.sleasman@gmail.com)
Wentworth Institute of Technology, Boston, MA
Electromechanical Engineering

***Abstract*— In an ever-adapting world, renewable energy resources are becoming increasingly relied upon for modern life. The rapidly expanding industry of wind energy, which has come to dominate this sector in production and versatility, suffers from turbines which face catastrophic blade failures and high maintenance costs. Many new projects are being developed to prevent, detect, and mitigate damage to turbine components to combat these issues. While there are several tools which actively determine turbine blade damage, there are currently no widely used systems to monitor the blades remotely and consistently during operation. This project proposes an inexpensive strain measurement array, comparable to lab equipment, which can collect data for the inverse finite element method and detect damage. The basic system designed could be incorporated into a turbine's supervisory control and data acquisition to decrease turbine downtime, improve operational safety, and extend the lifespan of wind turbine blades, reducing maintenance costs and improving sustainability within the wind energy industry.**

I. Introduction

Wind, as a renewable energy resource, is becoming more common, but its increased use for grid power generation drives rapid development where some design factors lag. Wind turbines have high maintenance costs, crew safety issues, end-of-life concerns, and failures. Operational and Maintenance (O&M) costs account for roughly one-third of a wind farm's total lifecycle expenses, with annual costs for land-based turbines ranging from $30–$57/MWh, and offshore turbines from $52-$184/MWh [1]. To improve the viability of grid-scale wind power, the levelized cost of energy (LCOE) can be reduced by innovating O&M processes and technology [2]. Through industry research, site visits at The Wind Technology Testing Center (WTTC) [3], and consultation, it was determined that while wind turbine systems face issues within gearboxes, generators, and structural elements, blade failure remains one of the most critical and costly concerns for operators (Table 1) [4].

Wind turbine blades operate under continuous aerodynamic loading, complex cyclic stresses, and harsh environmental exposure, making them prone to gradual degradation and sudden failure. Common root causes include manufacturing defects, fatigue cracking, lightning strikes, and leading-edge erosion [5], [6]. Failure of a single blade can result in significant downtime and costly repairs (Table 1) [4] with replacements often requiring heavy-lift vessels or specialized cranes that can add hundreds of thousands to repair costs [6]. Modeling from IEA Wind TCP Task 26 and WOMBAT studies shows that even a 10–20% increase in mean time between failures can save millions over a wind farm's lifetime [1], [7]. As reported by Hsu et al. (2020) [8], early fault detection is critical because unplanned outages drive substantial operational expenditure and reduce energy production. Predictive maintenance approaches, leveraging sensor data and advanced analytics, can extend asset lifetimes and improve availability.

Turbine monitoring systems are primarily designed for drivetrain components and are often connected to Supervisory Control and Data Acquisition (SCADA) systems. Structural health monitoring (SHM) for blades is missing from this system [9]. Strain measurement provides a direct indicator of structural deformation, which can be correlated to damage initiation and growth. According to the National Renewable Energy Laboratory (NREL) testing protocols, validating such systems requires accurate, repeatable measurement under representative loading conditions to ensure they can perform reliably in the field [10]. Strain-measure has an advantage over other techniques in its compatibility with inverse finite element method (iFEM), a software technique to determine stress and damage from model deformation. Blade SHM is a clear next step for the wind energy industry, and strain measure is possibly the strongest candidate.

TABLE I. BLADE REPLACEMENT COSTS THOUSANDS OF USD

Damage	Location	Material	Labor	Access	Total
Minor	Onshore	3	7	15	25
	Offshore	3	7	30	40
Major	Onshore	8	40	68.4	116.4
	Offshore	8	40	114	162
Replacement	Onshore	35 – 60	50 – 80	109 – 200	194 – 340
	Offshore	35 – 60	50 – 80	309 – 481.5	394 – 721

II. Purposes and Objectives

To increase the global share of wind energy, the simplest approach is to reduce the LCOE. Maintenance and end-of-life costs for wind turbines blades are far from optimized. Early detection of damage and structural stress is essential to lowering operational costs and extending service life. The strain gauge array (SGA) monitoring system in this paper is designed to be installed on wind turbine blades in the factory and in the field to reduce the LCOE and improve safety. This project intends to optimize the following objectives:

- Ease of installation to increase accessibility
- Optimal user experience and training requirements
- Minimal footprint on a blade's operation
- Compatibility with SCADA and turbine hardware
- Environmental resilience
- Endurance for longevity and reusability
- Effectiveness in tracking damage, stress, and fatigue
- Design for manufacturing to reduce lead times

I. Design

A. Hardware

Panel: The panel refers to the outermost circuit of the design. These units connect to eight strain gauges and interpret analog readings into inter integrated circuit (I2C) serial data; therefore, this circuit is critical for the system's accuracy and precision. Thermal factors and manufacturing tolerance must be minimized, as seen with the chosen components in appendix A.

Strain gauges are connected to a Wheatstone bridge in the panel using the three-wire configuration. They are connected through two multiplexers (MUXs) in quarter bridge formation. The schematic shown in Fig. 1 [11] allows for these connections through screw and solder wire connectors (J2-J4). MUXs (U5, U8) and solid-state relays (SSRs) (U6, U9, U11) are controlled by the I2C port expander 'U7'. When reading a strain value, the multiplexers are enabled and addressed, SSR 'U9' is closed to provide power, and SSRs 'U6' and 'U11' are open. During calibration, after a zero value is read from each strain gauge, the MUXs are disabled and SSRs 'U6' and 'U11' close to connect the shunt resistor 'R4'. This allows for gain correction to be calculated (1) by comparing a lab expected strain (ε_E) with the system measured strain and zero point (ε_M and ε_0). The voltage difference of the Wheatstone bridge is realized and amplified by the instrumentation amplifier (IAMP) 'U3' and then processed by the analog to digital converter (ADC) 'U4'. The recorded value is a 16-bit signed integer which can be read through the I2C bus.

$$K = \frac{\varepsilon_E}{\varepsilon_M - \varepsilon_0} \tag{1}$$

Apart from the I2C bus, all systems on the panel are powered with a precision 5-volt reference (U2). While most errors in the system are expected to be consistent (i.e. resistor tolerance, integrated circuit (IC) imprecision) or predictable (i.e. thermal effects), voltage error cannot be accounted for in software. Therefore, this precise IC was chosen.

Connection: Hardware components of the design are connected through I2C protocol, providing simple operation by the microcontroller. To resolve I2C's short range, buffers (Fig. 2 [11], U1) are used between the panel and the expander modules to isolate the transmission line and increase the electromagnetic interference (EMI), voltage, capacitance, and current limits of the serial channel. The limiting factor of the transmission is capacitance, which reduces maximum signal frequency. The buffers allow a maximum of 4000 pico-farads

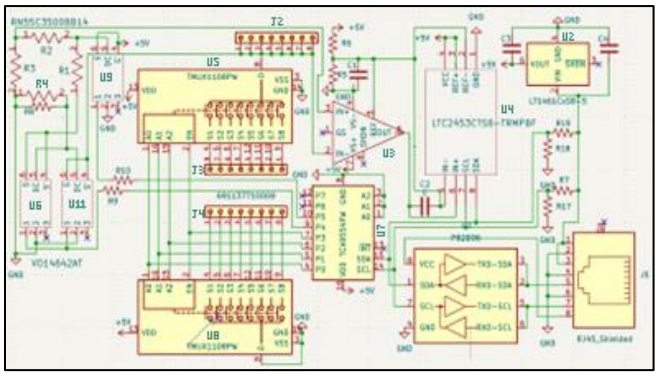

Figure 1. Panel Electrical Schematic.

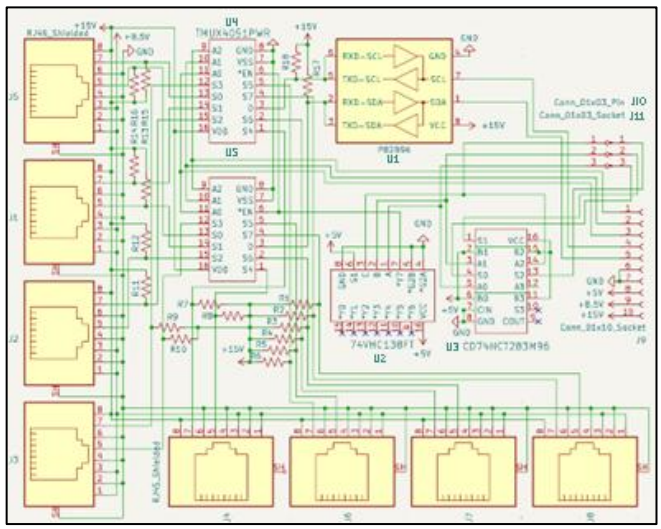

Figure 2. Expander Module Electrical Schematic.

along the transmission line. CAT6 cable was selected for its 52 pico-farad per meter capacitance [12] allowing up to 75 meters of range for the system and installation on the first half of all current wind turbine blades. Shielded variety is preferred.

8.5 volts are sent to the panel because the 5-volt reference requires 7.5+ volts to provide its maximum current of 50 milliamps, and, at this current, the voltage received by a panel at ~75 meters would be ~1 volt lower than supplied for a cable with 100 ohms per meter (with 2 parallel 8.5 volt supplies and 3 parallel grounds).

Expander Modules: The expander modules are connected on an eight-by-eight rack at the base of the blade and connect to the central microcontroller. Each module splits a single I2C bus into eight buffered buses using MUXs 'U4' and 'U5' as seen in the schematic Fig. 2. Each column of modules is connected to an isolated I2C bus from the central controller, allowing individual operation. The analog MUXs in each module are enabled by a decoder (U2) connected to the general-purpose input-output (GPIO) pins from the microcontroller. As the signal is passed down through modules in a column, the four-bit adder 'U3' decrements the value such that modules in different rows are connected by different addresses. In these ways, every module in the grid is isolated. Modules stack via a 10-pin socket header with long pins. The row isolation hardware uses three surface mount sockets and three surface mount pins directly opposite each other. The sockets of the first module connect to a ribbon from the central board.

Central Components: An ESP32-DEVKIT microcontroller runs the system, chosen for its availability. While no schematic is currently developed, the necessary properties of the central controller are defined. The controller must provide up to 1 amp at 15 volts, up to 5 amps at 8.5 volts, and 5 volts for running itself and the modules. The circuit will be connected to the turbine hub's power and data using standard slip rings. It uses a TCA9548A I2C breakout chip to create eight isolated channels for the modules. Six of the ESP32-DEVKIT's GPIO pins are connected to address the modules. The central circuit will contain a thermometer

accounting for temperature effects on the circuitry. Future testing may show this single sensor is not adequate for temperature differences along the blade due to aerodynamic cooling, sunlight, or other factors.

B. Software

The first layer of software is written in the C++ programming language with the PlatformIO extension in Microsoft Visual Studio Code [13], [14]. Running on the ESP32-DEVKIT as the microcontroller, the software can measure strain, compensate data, and send formatted values to a connected computer. This software layer directly controls all MUXs to select strain gauges, as well as reading ADC values and managing SSRs on panels.

All output values are fully compensated by software and formatted to identify them with the strain gauge they connect to. Incoming ADC values (N_{ADC}) are converted to voltage difference based on the expected supply (V_s) and reversed through the operations of the IAMP (2). To convert to voltage, the raw ADC value must be divided by its resolution. This voltage is interpreted into a resistance change based on the Wheatstone Bridge equation (3) and expected circuit resistances (4). Finally, this value is converted to micro strain (5) by dividing the gain factor (G_f) and the neutral gauge resistance. This raw measurement is compensated to produce the final measurement during normal operation (6). Often several raw measurements are averaged before compensation to reduce error from noise.

$$\Delta V = \frac{N_{ADC} \times V_S}{50(2^{16}-1)} \tag{2}$$

$$R_4 = R_3 \frac{R_2 V_S - (R_1+R_2)\Delta V}{R_1 V_S + (R_1+R_2)\Delta V} \tag{3}$$

$$\Delta R = 354.02 \frac{1750-700\times\Delta V}{1750+700\times\Delta V} - 354.02 \tag{4}$$

$$\mu\varepsilon = \frac{\Delta R \times 10^6}{350 G_f} \tag{5}$$

$$\mu\varepsilon_c = (\mu\varepsilon - \varepsilon_0) \times K \tag{6}$$

The data can be stored and accessed from the second software layer on the user's computer. This data could be connected to a SCADA system. This software includes user interface, database functionality, and basic analysis tools. Finally, the data can be run in iFEM software packages with the manufacturer's models of the blade to determine damage, stress, fatigue, or other properties of interest.

C. Installation

The system is designed to be installed by technicians in the field or during manufacturing. The installation is non-invasive and has no effect on the structural integrity of the blade. First, the central controller and module rack are installed at the base of the blade or in the turbine hub. All required modules can be installed in the rack. All gauges can be glued onto the blade in designated locations based on the manufacturer's design specifications and 3D modeling. At this point, panels can be glued to the spars of the blade and connected to the module rack with CAT6 shielded cable. This cable should be permanently taped or glued to the surface of the blade to avoid stress during operation. Lastly, strain gauges are connected one at a time to the system, and their placement is mapped to the virtual model carefully. This ensures simulations are accurate. After strain gauge leads are screwed into the panel, and their position are confirmed in the software, they should be soldered to ensure good connection and prevent detachment. Strain gauge lead wires should similarly be taped or glued to the surface of the blade.

Once properly secured and powered, the ESP32-DEVKIT should be connected to software on a remote computer to interface the data it collects. On first startup, the system needs to be zeroed. Each blade of the turbine must be zeroed in a rest position. One recommended technique is to offset the zero measured on a static blade with the expected load at the blade angle from simulation. Simpler techniques may be possible in a manufacturing environment.

II. Evaluation

The design described in the previous section outlines the conceptual work completed to address some of the current issues in wind turbine blades. To evaluate the principles of the proposed system simulations were run, and a small prototype was constructed to meet the time and budget constraints of the paper. Several tests were conducted to verify the effectiveness of the hardware.

A. Simulation

Two primary tools were used to simulate the system for hardware design. A Simscape (MATLAB Simulink) [15] model (Fig. 3, Fig. 4) was designed to verify the ideal circuit setup and is a simplified version of the panel design. This simulation operated without error and could therefore determine whether the pure mathematics of the system were

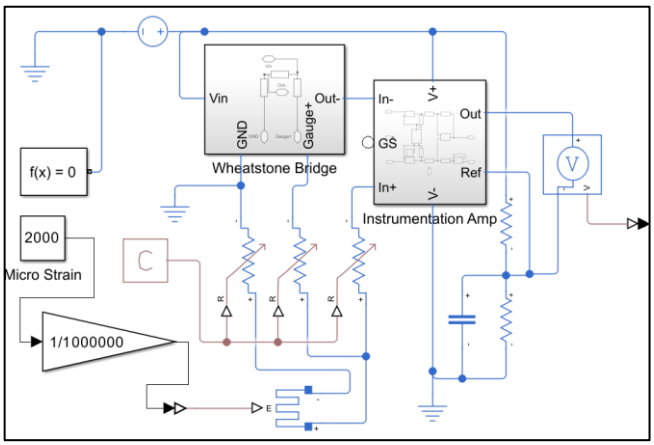

Figure 3. Ideal Analog Circuit Simulation in Simscape [15]

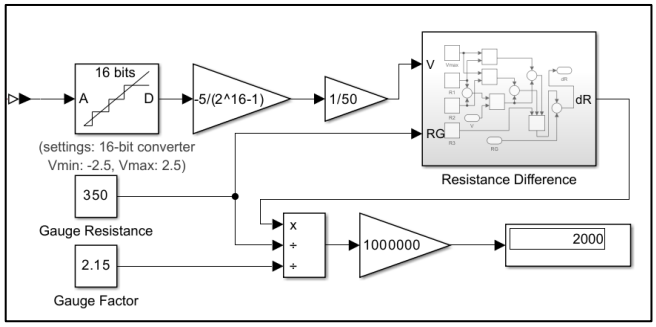

Figure 4. Ideal Software Simulation in Simulink [15].

correct during design. The second tool was a graphing calculator model utilizing Desmos [16]. This model was used to determine the expected error of the system with all components added, which assisted in the selection of parts for the design and adherence to the 0.5 micro strain precision target [3].

B. System Prototype

The prototype for this system as seen in Appendix B was constructed on breadboards using available lab equipment. The entirety of the panel design was implemented on a single board, except for the screw wire connectors. Strain gauge leads were inserted directly into the breadboard. This was connected through a 10-meter shielded CAT6 cable to a secondary breadboard which contained a simplified central circuit (expansion modules were not implemented for testing). The software for testing was simplified to calibrate on startup and not accept user input. A robust data storage system is not yet developed. This prototype allowed for the verification of circuit design, minor modifications, and clarity for ICs usage and behavior. Additionally, it allowed the running of basic system testing to compare results with simulations and expected results.

C. Transmission

I2C protocol requires a strong connection between the central controller and target components along the communication bus. Testing was conducted to ensure the buffered I2C bus worked without any sign of transmission errors as sending and receiving data is the basis of the operations for this project. Over the course of 30 seconds, constant instructions were sent to the circuit, and data was returned for several trials. This operation was conducted on the full prototype over a 10-meter CAT6 cable. Transmission errors can occur when there is an interruption in connection to central computer, faulty circuit wiring of the I2C bus, or computer not being able to process the incoming signal. The software will print an error message if one occurs and none were observed during testing. This proves the circuit's ability to consistently provide effective communication.

D. Thermal Properties

It is known that strain gauges and all other electronics devices operate slightly differently at different temperatures. In this experiment, the gauge was held at a steady strain value while the prototype provided current and took measurements. Thermocouples were used to track the temperature of both the 5-volt reference and the strain gauge. The experiment also tracked the output voltage of the reference chip, but these results were recorded as a constant after no change was observed. The 5-volt reference was paired with a small aluminum heat sync. Due to technician limitations, temperature measurements were taken every 10 seconds. As expected, the measured strain corelated with the gauge temperature (Fig. 5). There was significant overall temperature change due to the gauge being placed on a glass fiber reinforced composite (GFRC) sheet, which is the material used in wind turbine blades. GFRC is more insulative than other common materials.

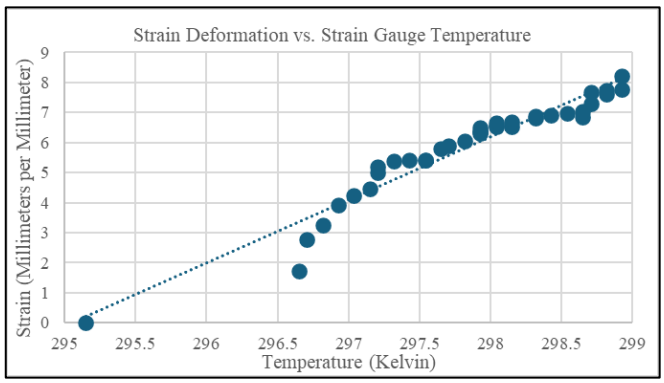

Figure 5. Temperature Effect on Strain Gauge Measure

E. Measurement

The most important system test used a cantilever beam and micrometer to determine strain measurement accuracy and precision. This test connected the prototype to a strain gauge glued to a steel beam giving the results shown in Fig. 6. The specific properties of the steel beam were determined to be inconsequential as they were not present in the final derived formula for cantilever strain (7) where h is the beam thickness, δ is the micrometer displacement, L is the beam length from clamp to bending micrometer, and x is the position of the strain gauge from the clamp. This equation assumes elasticity and moment of inertia are constant in the beam. It should be noted that neither L nor x includes the portion of the beam in the clamp.

$$\varepsilon = \frac{3h\delta}{2L^3}(x - L) \tag{7}$$

Three trials were conducted consecutively. For the first trial, the system gain was manually calibrated in software. Each trial was zeroed at the beginning of the run. Measurements were taken every 1.27 millimeters (0.05 inches) from 0 to 17.78 millimeters (0.7 inches). After these trials, a series of measurements were taken in the same manner except the system used its automatic shunt resistor calibration method. Fig. 6 shows these results. While the manual calibration has an error of 0.9%, the automatic calibration has an error of 21%.

III. Concluding Remarks

A. Evaluation Review

Transmission behavior of the prototype was exceptional. Unexpected or unexplained errors were not observed either

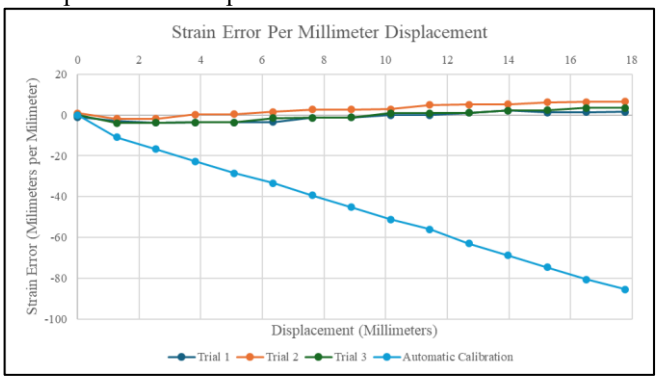

Figure 6. Error of Manual and Automatic Calibration

during official tests or throughout the time the system was being used. Some results from the temperature test were in line with expectations. Using a heatsink, the 5-volt reference heated by only ~3 degrees Celsius. No change was observed in output voltage. Temperature effects on strain measurement show a non-linear curve. More testing is required to determine the cause of this, but some possibilities are capacitance or warmup of system components. As strain gauges are intended to be connected and measured for only a short, this unexpected result is non-trivial and must be addressed through future testing. The system must operate over a wide range of temperatures influenced by weather and ambient air.

The cantilever experiment to validate strain measurements showed some good behavior and some system weak points. While manually calibrated, the system worked exactly as intended, showing precise and accurate results. Unfortunately, the automatic calibration had unacceptable error. While this may be due to a flawed design, some other parameters need to be accounted for first. Because the system was installed on a breadboard, the resistance of the shunt circuit would not be nearly as precise as expected and would not correlate properly with the strain circuit. To account for this factor, the system needs to be tested on a printed circuit board (PCB). The other main factor is heating. The experiment was conducted at equilibrium temperature for simplicity, and this is not in the prototype software. These factors should be accounted for before a redesign of the gain calibration system. The original testing plan involved validating strain gauge performance against an Instron universal testing machine in accordance with ASTM D3039 [17], but this machine was found to have insufficient resolution for proper testing.

TABLE II. ESTIMATED SYSTEM COST BREAKDOWN

Estimated System Cost for a 70-Meter Turbine Blade			
Hardware			
Element	Count	Cost	Total[a]
Panel	60	$38.00	$2280.00
Components		$28.00	
Manufacturing		$10.00	
Module	8	$26.00	$208.00
Components		$16.00	
Manufacturing		$10.00	
Controller	1	$246.00	$246.00
Components		$36.00	
Manufacturing		$10.00	
Module Rack		$200.00	
CAT 6 Cable	1050	$0.80	$840.00
Strain Gauges	420	$20.00	$6000.00
Adhesives			$110.00
			$9474.00
Shipping			
			$200.00
Installation			
Operation	Count	Hours	Total[b]
Gauges	420	0.25	105
Panels	60	0.5	30
Central	1	1	1
Software Integration			4
Other			12
	× 30		$4560.00
Raw Total	Overhead Factor		Total
$14234.00	1.25		$17792.50

a. Component costs estimated from values in Appendix A and the DigiKey Catalogue [12]

b. Other values are an aggressive estimate based on industry knowledge of the authors.

B. *Estimated Cost and Impact*

At production scale, the system is projected to cost approximately 18,000 dollars (Table 2) per 70m blade, an approximately average length, including sensors, electronics, and labor. Refinement of the design (reducing the number of required sensors and simplifying installation) has the potential to lower costs considerably. In the context of maintenance costs, where minor blade repairs can exceed this cost, and where heavy lift mobilization can add hundreds of thousands of dollars to a repair, the ability to prevent a failure or extend a blade's service life by several years would offset the investment (Table 1) [4]. Beyond direct cost recovery, early detection of structural issues reduces unplanned downtime, thereby increasing annual energy production and improving overall capacity. Over the lifetime of a turbine, these operational gains compound to yield substantial farm-level savings, particularly when applied across large fleets. The system's modular architecture supports reuse when blades are retired and enables retrofitting without major structural modifications. Operators can integrate the technology into current maintenance strategies with minimal disruption. This combination of cost efficiency, performance benefit, and deployment flexibility positions the design as a viable pathway for improving asset longevity, reducing LCOE, and enhancing the long-term sustainability of wind power operations.

C. *Future Work*

The small size of key components, including the INA351 (IAMP) and LTC2453 (ADC), required precision soldering, making assembly quality critical for overall system accuracy and reliability. Future development should address these constraints by moving to PCBs to reduce parasitic resistances and wiring inconsistencies. Circuit housing should implement shielding, filtering, and protection against environmental factors. Central circuit and expansion modules should be fully designed and tested thoroughly. Future work should consider replacing expansion modules entirely with a transmission protocol capable of connecting panels in series instead of parallel. While CAT6 cable has EMI protection, gauge lead wires should be tested for EMI and static sensitivity.

On the software side, refining compensation algorithms, incorporating automated calibration, and optimizing processing speed and error handling will further enhance performance. A graphical user interface will provide intuitive operation, clear data visualization, and easy export.

Once these steps are completed, testing at a full-scale facility such as WTTC and using the system for iFEM will be crucial to determining the system's capabilities and future steps, especially if it is to be integrated with SCADA. Data collected in the field may also encourage additional cooperation between designers and wind farms, pushing the industry towards better blade construction.

APPENDIX

A. Trade Analysis

Selected parts are to be available and stocked on DigiKey [12] or at Wentworth laboratories, be voltage and current compatible (5 volts, or 15 volts for buffer bus), have low tolerance, have wide temperature operability, be in a larger package when possible, be I2C compatible (when relevant), and be low cost when possible. Specific attributes for selection are listed in Table 3 [12].

TABLE III. MAJOR COMPONENETS ATTRIBUTES AND COST

PART (Attributes)	Price (USD) 1 (1000)	Description	Count (Parent)
ESP32-DEVKITC	10.00 (10.00)	Microcontroller	1
Documentation, high level control, Wi-Fi			Central
RN55C3500 BB14	1.49 (0.50643)	Resistor	4
350 Ohm 0.1%. Low temperature sensitivity			Panel
LTC2453	5.27 (1.9125)	ADC	1
16 bit, 60 samples/sec, external reference			Panel
INA351CDS	0.66 (0.31173)	Instrument. Amp.	1
Gain: 50, buffered reference			Panel
LT1461CIS8-5	7.67 (3.20)	Power Supply	1
0.08% voltage variation. Wide input range.			Panel
TCA9548A	1.41 (0.71927)	I2C Mux	1
Convenient package, ease of use			Central
TMUX1108	3.97 (2.42504)	Analog Mux	2
Low resistance, port count (8)			Panel
TCA9554	1.35 (0.68734)	I/O Expander	1
Port count (8), ease of use			Panel
VO14642AT	2.09 (1.47482)	Solid State Relay	3
Low resistance			Panel
P82B96P	5.22 (2.99425)	I2C Buffer	1 (1)
Common usage, no software			Module (Panel)
TMUX4051	0.56 (0.26111)	Analog Mux	2
Low capacitance, port count (8)			Module
74VHC138FT	0.33 (0.14840)	Decoder	1
Active low, input count (3)			Module
CD74HCT 283M96	0.69 (0.33507)	Binary Adder	1
Number of bits (4)			Module

B. System Prototype

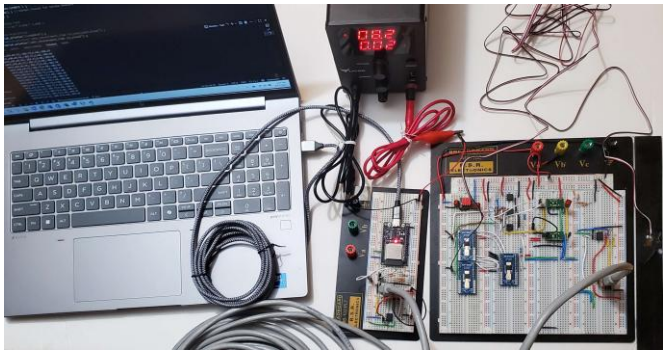

Figure 7. System Prototype.

ACKNOWLEDGMENT

The Team sincerely thanks Professor James McCusker and Program Director Afsaneh Ghanavati for support and funding, Connor Read at the Wind Turbine Testing Facility for industry knowledge, and Associate Professor Marisha Rawlins for software guidance.

REFERENCES

[1] G. Smart, A. Smith, E. Warner, I. Bakken, B. Prinsen, and R. Lacal-Arántegui, "IEA Wind Task 26: Offshore Wind Farm Baseline Documentation," U.S. Department of Energy. Accessed: Feb. 20, 2025. [Online]. Available: https://docs.nrel.gov/docs/fy16osti/66262.pdf

[2] Kikuchi, Y.; Ishihara, T. Availability and LCOE Analysis Considering Failure Rate and Downtime or Onshore Wind Turbines in Japan. Energies 2021, 14, 3528. https://doi.org/10.3390/en14123528

[3] A. Aster, G. Perez, and E. Sleasman, "Interview with Connor Read, Test Engineer at Wind Technology Testing Center, Boston, MA," Feb. 21, 2025. Available: https://github.com/GSPerez999/WindTurbineStrain/wiki/Interview-with-Connor-Read,-Wind-Technology-Testing-Facility,-Boston,-MA

[4] L. Mishnaevsky Jr. and K. Thomsen, "Costs of repair of wind turbine blades: Influence of technology aspects," June 2020, doi: 10.1002.

[5] L. M. Jr, "Root Causes and Mechanisms of Failure of Wind Turbine Blades: Overview," 2022, doi: 10.3390/ma15092959.

[6] Song, X.; Xing, Z.; Jia, Y.; Song, X.; Cai, C.; Zhang, Y.;Wang, Z.; Guo, J.; Li, Q. Review on the Damage and Fault Diagnosis of Wind Turbine Blades in the Germination Stage. Energies **2022**, 15, 7492. https://doi.org/10.3390/en15207492

[7] R. Hammond and A. Cooperman, "Windfarm Operations and Maintenance cost-Benefit Analysis Tool (WOMBAT)." Oct. 01, 2022.

[8] J.-Y. Hsu, Y.-F. Wang, K.-C. Lin, M.-Y. Chen, and J. H.-Y. Hsu, "Wind Turbine Fault Diagnosis and Predictive Maintenance Through Statistical Process Control and Machine Learning," vol. 8, p. 23427, 2020, doi: 10.1109/access.2020.2968615.

[9] K. Leahy, C. Gallagher, P. O'donovan, and D. T. J. O'sullivan, "Issues with Data Quality for Wind Turbine Condition Monitoring and Reliability Analyses," vol. 12, no. 2. in Energies, no. 12, vol. 12. MDPI AG, Jan. 09, 2019. doi: 10.3390/en12020201.

[10] M. Desmond, S. Hughes, and J. Paquette, "Structural Testing of the Blade Reliability Collaborative Effect of Defect Wind Turbine Blades." June 01, 2015.

[11] KiCad, KiCad Development, vol. 3. 2025.

[12] DigiKey, "Product Index." Accessed: Aug. 06, 2025. [Online]. Available: https://www.digikey.com/en/products

[13] *PlatformIO*. PlatformIO Labs, 2025.

[14] *Visual Studio Code*, vol. 1.103. Microsoft, 2025.

[15] MATLAB, Simulink, and Simscape. The MathWorks, Inc., 2025.

[16] Desmos. Desmos Studio, PBC, 2025.

[17] "Standard Test Method for Tensile Properties of Polymer Matrix Composite Materials." in ASTM. ASTM International, June 04, 2014. doi: 10.1520.